Applied Cardiopulmonary Pathophysiology 16: 212-225, 2012

Electrical impedance tomography: New diagnostic possibilities using regional time constant maps

R. Pikkemaat[1], K. Tenbrock[2], S. Lehmann[2], S. Leonhardt[1]

[1]Philips Chair for Medical Information Technology, RWTH Aachen University, Aachen, Germany; [2]Department of Pediatrics, Dept. of Pediatrics, University Hospital, RWTH Aachen University, Aachen, Germany

Abstract

Pulmonary function tests are used to assess the severity of obstructive and restrictive lung diseases. These tests provide information on the whole lung considered as one compartment and can be used to globally describe the physical properties of flow resistance *R* and compliance *C*, but do not yield regional information. Electrical impedance tomography (EIT) is widely used in clinical research regarding ventilation monitoring. In this study, EIT recordings were performed simultaneously with spirometry during a forced expiration maneuver. We could show that EIT provides similar results to describe pulmonary mechanics. Therefore, seven patients (8-14 years) with asthma bronchiale were examined before and after therapy with Salbutamol to perform broncho spasmolysis. We found a relation between flow resistance R and global time constant τ_{global} with positive correlation r=0.88. Additionally, we propose the use of the regional time constant $\tau_{reg}(x)$ (RTC-map) as a new imaging modality in a case study which demonstrates its performance considering broncho spasmolysis.

Key words: asthma bronchiale, diagnosis, electrical impedance tomography, pulmonary function test, time constant

1. Introduction

Electrical impedance tomography (EIT) is a relatively new technique in which a tomogram is created that maps the distributed electrical impedance within one slice of a body to a 2D image [1]. Since the electrical impedance of pulmonary tissue is strongly dependent on the air content of the alveoli [2], the technique can be used to monitor not only global but also regional ventilation of the lung [3-5]. Due to its ability to produce tomograms at a rate of 40-50 frames per second, EIT can monitor regional ventilation with extremely high dynamics [6]. Some approaches even aim at beat-to-beat cardiovascular monitoring using EIT [7-9]. Here, however, we propose to use EIT for regional diagnosis of obstructive lung diseases during pulmonary function tests.

Most classical methods used to assess the mechanical properties of the lung and, thereby, to diagnose certain diseases are based on spirometry [10]. However, in contrast to EIT, spirometric methods only provide data on global parameters [11, 12] and do not allow quantitative examination of regional pathology in lung tissue. To remedy this, we propose

the use of EIT for regional pulmonary function tests (PFT). Using EIT, equivalents to classic parameters such as forced expired volume after 0.5s ($FEV_{0.5}$), forced expired volume after 1.0s ($FEV_{1.0}$) and functional vital capacity (*FVC*) can be defined both globally and regionally.

Although different tomographic techniques (e.g. CT, MRI) can be used to assess the regional mechanical status of lung tissue, see [13], this requires considerable technical effort. Moreover, because these modalities lack the same speed of regional data acquisition as EIT, they are unable to provide data based on flows or volumes at certain time points during a maneuvers, e.g. such as $FEV_{1.0}/FVC$ or forced expiratory flow at 25% of *FVC* (FEF_{25}), etc. Therefore, new diagnostic possibilities arise when using an EIT device that provides fast and accurate evaluation of regional pathology.

We propose a new method to evaluate the regional mechanical properties of pulmonary tissue. To rate the pathological state, the concept of regional time constant maps is introduced. Here, the regional time constant $\tau_{reg}(x)$ describes the product of local flow-resistance and local compliance in the respiratory system. In addition, using a case study, we report on the relation between τ (regional and global) and the classical parameters used in clinical practice.

2. Materials and methods

2.1 Electrical impedance tomography

Commonly used EIT devices have 16 or 32 electrodes. In this work we use the *EIT Evaluation Kit 2, EEK2,* Draeger Medical GmbH, Luebeck, Germany which is an 16-electrode EIT system. In thoracic EIT the electrodes are placed equidistantly around the chest within an even plane. The principle of data acquisition can be described as a multi-directional four-point measurement of the electrical impedance. For this, two adjacent electrodes drive an alternating current while all pairs of the remaining electrodes are used to measure the resulting surficial voltages. In an N=16 electrode EIT, N-3=13 linearly independent voltages are measured. Subsequently, the next pair of electrodes is chosen to drive the current and, again, 13 linearly independent voltages are measured (Figure 1).

The whole procedure continues until each adjacent pair of electrodes has been used to inject currents. Finally, 16*13=208 voltages are acquired; however, only half of them are linearly independent due to the principle of reciprocity. Merging all voltages in a vector v_n with n denoting the point in time (number of frame), the tomogram Z_n (vector containing all pixels) can be calculated by

$$Z_n = B \cdot v_n \qquad \text{(eq 1)}$$

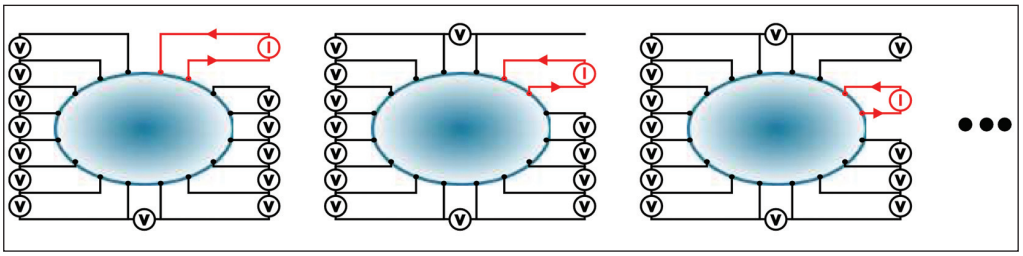

*Figure 1: Data acquisition in EIT: subsequent injection of alternating currents between all adjacent pairs of electrodes. All adjacent surficial voltages are measured simultaneously between electrodes not driving a current. Finally (16*13)/2=104 linearly independent voltages are acquired, which are subsequently used to calculate a tomogram depicting the regional distribution of electrical impedance.*

in which B describes the reconstruction matrix. Although the reconstruction of EIT is a non-linear inverse problem, (eq. 8) shows a linear approach of reconstruction. Due to ease of use and fast calculation (i.e. a simple matrix multiplication), this linear approach is used in most practical implementations [14]. Thus, currently used devices can deliver up to 50 images per second and capture very fast dynamics. To generate B, different approaches are used, e.g. filtered back-projection [15, 16], one-step linear Gauss-Newton solvers [17, 18] or model based calculations [14].

Although the technique is called EIT, it appears that reconstruction of absolute regional impedances is difficult and demands considerable information [19], e.g. accurate positioning of the electrodes. Therefore, a relative imaging modality has been devised in which relative voltages Δv_n are used instead of v_n. The relative voltages Δv_n are defined using a reference v_{ref}, e.g. mean or minimal voltages of a certain period of time. They are given by

$$\Delta v_n(i) = \frac{v_n(i) - v_{ref}(i)}{v_{ref}(i)} \qquad \text{(eq. 2)}$$

and subsequently yield to relative impedances ΔZ_n with

$$\Delta Z_n = B \cdot \Delta v_n \qquad \text{(eq. 3)}$$

This relative imaging modality is referred to as *functional* EIT; by providing more stable tomograms this enhances the use of EIT in a clinical setup. The technique is already gaining importance in research on ventilation monitoring. Moreover, the recent introduction of an EIT device for clinical use (PulmoVista® 500, Draeger Medical GmbH, Germany) will probably increase the use and importance of EIT in clinical practice.

2.2 Spirometry and pulmonary function test

A spirometer is a measurement device to evaluate the gas-flow of a breathing patient. Spirometry is used for pulmonary function test (PFT), in which flow and volume measurements are used to diagnose and evaluate obstructive or restrictive pulmonary diseases. During one part of this test, the patient is asked to breathe in a defined course of action. First, the patient breathes normally for a short period of time to measure the usual tidal volume *TV*. Then, the patient is asked to inspire and expire maximally to assess the inspiratory and expiratory reserve volumes (*IRV* and *ERV*) and to estimate functional vital capacity (*FVC*), see Figure 2.

$$\text{FVC} = \text{IRV} + \text{TV} + \text{ERV}. \qquad \text{(eq. 4)}$$

These volumes reflect a patient's ability to ventilate their lungs, but do not necessarily reflect the local or global mechanical properties of pulmonary tissue. Some patients who suffer from a chronic airway disease develop an adapted physiology and body composition. For instance, over the years a chronic asthmatic patient may develop enhanced growth of breathing musculature, since constantly increased pulmonary flow resistance demands a higher expiration force. In this case, the patient may be able to breathe with increased strength thereby achieving almost the same *FVC* as a healthy subject. Because of this, the so called Tiffeneau test is often added to the routine spirometric measurements. The Tiffeneau test consists of a maximal inspiration followed by a forced expiration, which has to be performed as forcefully as possible (Figure 2, right).

Although this test seems to depend on the patient's cooperation, it has been shown that maximal flow stops increasing whereas the driving pressure continues to increase [20, 21, 22]. This phenomenon is often observed in patients suffering from an obstructive disease. This characteristic lung behavior

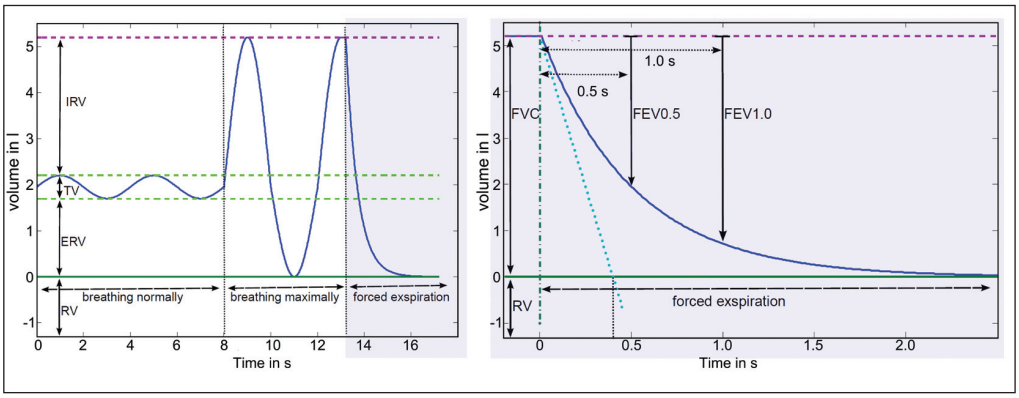

Figure 2: Left: Time course of lung volume during tidal breathing and during forced expiration. Right: a period of forced expiration on an enlarged scale over time; t = 0 s denotes the beginning of the forced expiration.

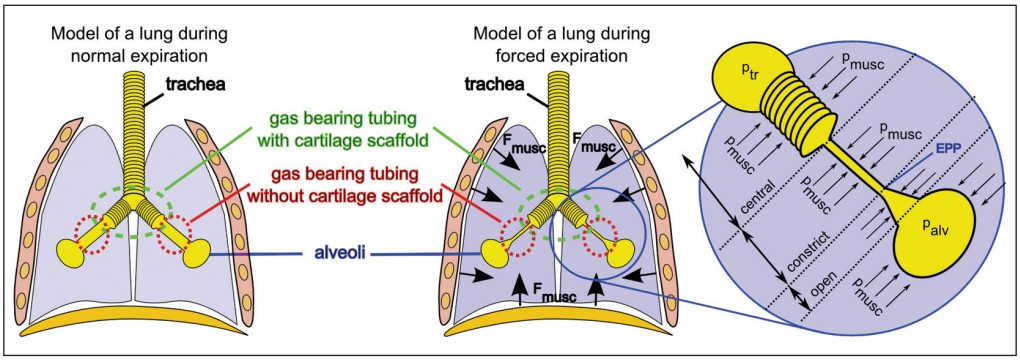

Figure 3: Principle of self-constricting bronchioles during forced expiration: the driving pressure decreases along the tubings during forced expiration. An equal pressure point (EPP) arises at which the intraluminal pressure equals the pressure of the surrounding environment. Between EPP and the non-collapsible respiratory tubings, a very narrow tube occurs which limits the expiratory flow. Thus, increasing intrathoracic pressure by enhancing the force of the musculature (p_{musc}) does not lead to increasing flow at high intrathoracic pressures.

is generally explained by the self-constriction of the collapsible bronchioles (Figure 3).

The alveolar pressure p_{alv} is given by the recoil pressures caused by the alveolar compliance and the pressure within the surrounding environment. Simplified, the pulmonary extra-luminal pressure is assumed to be the pressure applied by the breathing musculature p_{musc}. Since gas flow leads to a pressure drop along the tubing between alveoli (p_{alv}) and trachea (p_{tr}), an equal pressure point (EPP) [21] arises where the intra-luminal pressure is equal to p_{musc}. Towards the trachea, the bronchioles almost collapse resulting in a narrow tube that restricts expiratory flow. This „waterfall“ or „Starling resistor“ effect [20] causes a limited maximal flow which cannot be further increased by increasing muscular effort p_{musc}. This relationship ($\dot{V}_{ex} \neq f(p_{musc\text{-}ex})$) is derived in the section below. Thus, during forced expiration the measured flows and volumes are only slightly influenced by the expiratory musculature and, therefore, are hardly affected by the patient's cooperation. As long as constriction develops, the expiratory flow is only affected by the property of the bronchioles and the alveolar pressure at the point of maximal inspira-

tion.

Figure 2 shows that there are defined volumes describing the global dynamic properties of the lung (*FVC, $FEV_{1.0}$* and *$FEV_{0.5}$*) during the Tiffeneau test. The forced expiratory volumes after the first 0.5 s (*$FEV_{0.5}$*) and after the first 1.0 s (*$FEV_{1.0}$*) describe the volumes exhaled after the defined period of time (Figure 2). Since the total volume may vary in different patients, the ratio $FEV_{1.0}$/FVC becomes a meaningful benchmark to describe flow resistance in a patient's lung and thereby reflects the severity of obstructive disease (section Mechanical Model of the Respiratory System). Obstructive disease is diagnosed when the patient is unable to breathe out 80% or more of the FVC within the first second; i.e. ($FEV_{1.0}/FEV_{0.5}$) < 0.8.

Because of the self-constricting bronchioles, the process of forced expiration shows the same characteristic as a passive exhalation in which lung compliance shows no significant effect. Consequently, flow characteristics are dependent only on pulmonary flow resistance and thus provide benchmarks to rate obstructive disease.

2.3 Mechanical model of the respiratory system

The lung contains a complex gas-bearing system with up to 23 bifurcations, which finally branches off to around 300 million alveoli. Each tube in the respiratory system exhibits a certain flow resistivity (approximately proportional to ($1/r^4$) according to Poiseuille's law) and elasticity (usually called „compliance"). However, compliance of the gas-bearing respiratory system is relatively small compared to the elasticity of the alveoli. Therefore, many approaches to mechanical modeling of the lung neglect compliance of the respiratory tubing (and the compressibility of the air itself). Lung compliance is mainly based on the compliance of the alveoli. Accordingly, the tubular system is only described by various flow resistances. If self-constriction is taken into account, the behavior of the lung follows the mechanical model shown in Figure 4.

Since the structure of each regional mechanical model is the same and each region is assumed to be independent from the oth-

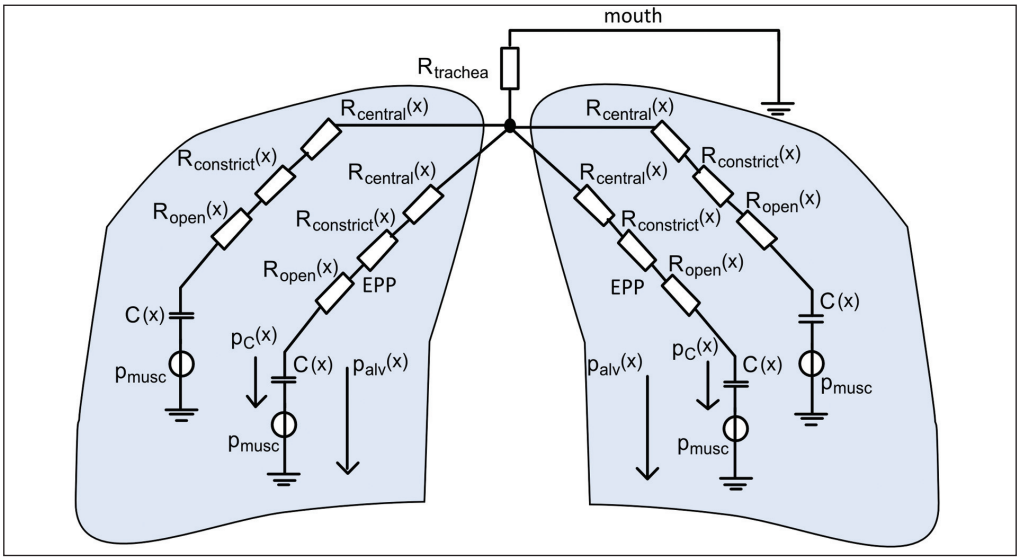

Figure 4: Mechanical model of regional peripheral pulmonary tissue during forced expiration. For simplification only two regions per lung are sketched, but the principle can be applied to any part of the lung. All areas of pulmonary tissueVkhme3 feature a similar structure, the core model. Since $R_{open}(x)$ and C(x) depend on the position, the dynamic behavior, $\tau_{reg}(x)$ varies accordingly.

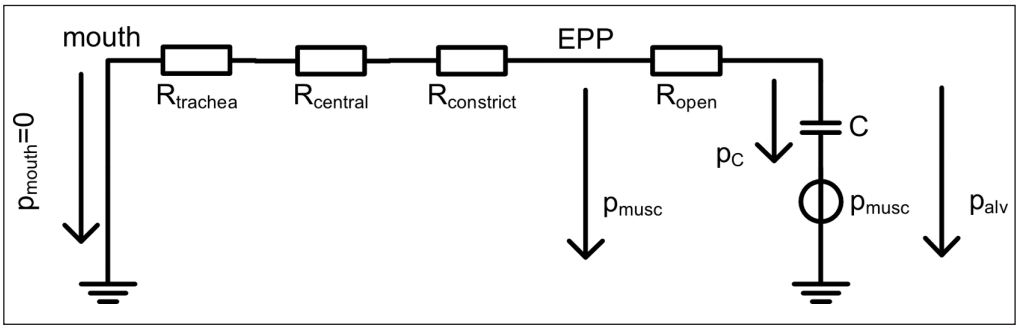

Figure 5: Mechanical core model of peripheral pulmonary tissue during forced expiration. The dynamics are influenced by the pressure p_c based on the reset force and the flow resistance of the open part of the tubing R_{open}, because of self-constriction. This core model can also be used for global analysis (e.g. τ_{global}) or for analysis of each individual region, e.g. $\tau_{reg}(x)$. (Note: In the remainder of the paper we will ignore the (x) identifier.

ers, we address local areas separately according to the core-model (Figure 5). This core model can be used to analyze all regional mechanical properties and can also be adapted for global analysis.

In the space between the *EPP* and the alveoli, because the intra-luminal pressure is higher than the pressure in the surrounding environment, the tubing is as open as possible. However, mucosal swelling or mucus can limit this opening. The reset pressure p_C at the very beginning of the maneuver is given by the inspiratory strength of the patient, because at maximum inspiration the elastic pressure pC is equal to the pressure of the inspiratory musculature. Since the maximum inspiratory force does not change during the procedure, the reset force can be assumed to be constant (in the same patient). Because of the self-constriction, $R_{constrict}$ causes a limitation in flow, i.e. the flow does not keep increasing when p_{musc} increases above a certain level. Consequently, the effective driving pressure is given by p_C and, therefore, the relative dynamic of the regional ventilation is only influenced by $C(x)$ and $R_{open}(x)$ for as long as the self-constriction persists. Hence, each region exhibits its specific time constant $\tau_{reg}(x)$. In general, each position in the lung is given by 3D coordinates. For simplification, we define $x:=(m,n)$ as a discrete 2D coordinate of the electrical impedance tomogram. Each EIT pixel maps a certain voxel of the 3D lung. With EIT the regional $\tau_{reg}(x)$ can be estimated separately for each pixel, based on the local change of impedance which correlates with the local air content.

Let the pressure caused by the breathing musculature p_{musc} be

$$p_{musc} = p_{musc\text{-}in} = const < 0 \qquad \text{(eq. 5)}$$

during the time of inspiration. Since flow stops at the point of maximum inspiration, we get

$$p_{alv} = 0 \Rightarrow p_C = - p_{musc\text{-}in} \qquad \text{(eq. 6)}$$

at $t = 0$ s. If now ($t = 0+$) the breathing musculature contracts as forcefully as possible and we assume that the expiratory force is constant during expiration, we get

$$p_{musc}(0+) = p_{musc\text{-}ex} = \text{const} > 0 \qquad \text{(eq. 7)}$$

$$p_{alv}(0+) = p_C^{(0+)} + p_{musc}^{(0+)} \qquad \text{(eq. 8)}$$

$$p_{alv}(0+) = p_{musc\text{-}ex} - p_{musc\text{-}in} \qquad \text{(eq. 9)}$$

at the very beginning of the forced expiration. According to the model in Figure 5, the expiratory flow $\dot{V}_{ex}$ is given by

$$\dot{V}_{ex} = \frac{1}{R_{open}} \cdot \left(p_{alv}(0+) - p_{musc-ex} - \int_{t'=0}^{t} \frac{\dot{V}_{ex}(t')}{C} dt' \right) \qquad \text{(eq. 10)}$$

$$\Rightarrow -\frac{p_{musc-in}}{R_{open}} = \dot{V}_{ex}(t) + \frac{1}{R_{open} \cdot C} \cdot \int_{t'=0}^{t} \dot{V}_{ex}(t')dt'. \quad \text{(eq. 11)}$$

This model predicts an exponentially decreasing volume and flow during the forced expiration which correlates with spirometrically measured values in clinical practice (compare the theoretically expected course of the lung volume in Figure 2 and real measured global impedance during forced expiration). This model yields an absolute lung volume V_{lung}

$$V_{lung}(t) = RV + FVC + e^{-t/\tau_{global}} \quad \text{(eq. 12)}$$

with $\tau_{global} = R_{open} \cdot C$ (eq. 13)

in which τ is the time constant that we are focusing on both globally (τ_{global}) and regionally ($\tau_{reg}(x)$).

In clinical practice, pulmonary dynamics are described by volume ($FEV_{0.5}$, $FEV_{1.0}$) or flow (FEF_{25}, FEF_{50}, FEF_{75}) whereas a characterization using the time-constant τ is commonly used in an engineering-oriented environment. Note that these parameters describe the same property, if a one-compartment mechanical model is used.

Since V_{lung} can be described by (eq. 12) (during forced expiration), the expired volume V_{ex} can be expressed as

$$V_{ex}(t) = FVC \cdot 1 - e^{-t/\tau_{global}}. \quad \text{(eq. 14)}$$

In clinical practice, since *FEV* is used to express the forced expired volume during a certain period of time, we define

$FEV_{1.0}$: = V_{ex} (t = 1.0 *s*) (eq. 15)

$FEV_{0.5}$: = V_{ex} (t = 0.5 *s*) (eq. 16)

In case of obstructive disease, clinically (FEV_{10}/FVC) < 0.7 to 0.8 is considered. This leads to $\tau_{global} \geq 0.6213$ *s* (in the case of 0.8). Generally, the time constant τ_{global} can be calculated from $FEV_{1.0}$ and FVC using

$$\tau_{global} = -1.0\ s \cdot \left[\ln\left(1 - {}^{FEV_{1.0}}/_{FVC}\right)\right]^{-1}. \quad \text{(eq. 17)}$$

Similarly, the time constant τ_{global} can also be calculated from $FEV_{0.5}$/FVC, and the forced expiratory flow (FEF) can even be used to estimate τ_{global}.

Although all parameters routinely used in the clinic ($FEV_{0.5}$, $FEV_{1.0}$, FEF_{25}, FEF_{50} and FEF_{75} in relation to FVC) can be calculated with the simplified model based on the FVC and τ_{global}, the parameters usually provide additional data that are useful for practical purposes. On the one hand this shows that the simplification is only valid up to a certain level of diagnosis; on the other, the way of determining τ_{global} needs to be carefully chosen depending on the main goal of the analysis.

2.4 Design of the clinical study

All patients were part of a human study which was approved by the local ethics committee (EK 118/10, 19th July 2010, University Hospital Aachen, Germany). In this study, patients (aged 8-14 years) with an assumed or known obstructive disease underwent a traditional pulmonary function test (PFT) in which medically relevant parameters, e.g. the respiratory flow resistance *(R)*, functional vital capacity *(FVC)*, forced expired volume after 1 s *($FEV_{1.0}$)*, etc. were assessed. During forced expiration maneuver (the Tiffeneau test), EIT data and the expiratory flow were recorded simultaneously.

EIT data were acquired with an EIT Evaluation Kit 2 (Draeger Medical GmbH, Luebeck, Germany), spirometric data with a Jaeger MS-IOS digital, and a Jaeger Bodyscreen II was used for body plethysmography (both Jaeger/Viasys/CareFusion, San Diego, USA). For EIT measurements a silicon electrode belt was used and attached to the body at the 6th intercostal space. Before performing the Tiffeneau test, global respiratory flow resistance was determined using body plethysmography.

Therapy (broncho spasmolysis) and all measurements were performed equally in each patient. All measurements (EIT, spirometry and body plethysmography) were performed twice, i.e. before and after lytic therapy with Salbutamol. To assure the effect of the drug, a waiting period of 10 minutes was arranged between both measurements. The relative change (percentage) in global impedance τ_{global} and R_{ref} were analyzed. Accordingly, in a given parameter 90% reflects a 10% decrease, 110% reflects a gain of 10% increase.

To show the validity of the mechanical model, τ_{global} and the EIT measurement itself in terms of PFT, we discuss the relationship between change in the spirometrically measured flow resistance R_{ref} and the time constant τ_{global} based on global impedance of the EIT data. Also, we introduce a new concept of visualization of regional lung mechanics called the „regional time constant map" (RTC-map). This concept is demonstrated using data obtained from an 11-year-old boy with a confirmed diagnosis of asthma.

2.5 Significance of EIT data streams in relation to PFT

It has been shown that changes in global electrical impedance within one tomogram correlate well with changes in gas content of the lung [23-26]. Based on these findings, global impedance is expected to correlate with pulmonary air content, excluding the residual volume (RV), see Figure 2. Since EIT delivers global and regional information about changes in electrical impedance, global and regional equivalents of $FEV_{0.5}$ and $FEV_{1.0}$ can be derived, namely $\Delta Z_{global\text{-}FEV1.0}$, $\Delta Z_{reg\text{-}FEV1.0}$, $\Delta Z_{global\text{-}FEV0.5}$ and $\Delta Z_{reg\text{-}FEV0.5}$ (Figure 6). For global considerations spirometry can be used as a clinically accepted reference. However, regional information derived from EIT cannot be compared with a gold standard

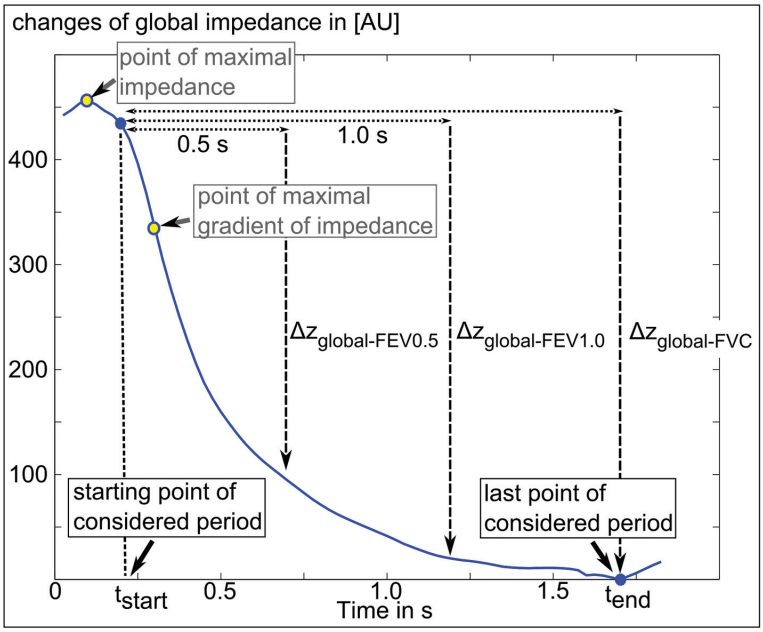

Figure 6: Global impedance during forced expiration: EIT equivalents of $FEV_{0.5}$ and $FEV_{1.0}$, i.e. $\Delta Z_{global\_FEV0.5}$ and $\Delta Z_{global\_FEV1.0}$, are defined according to the starting point t_{start}. The global time constant is calculated by fitting the measured global impedance to an exponentially sinking curve, as shown below. The regional calculations of $\Delta Z_{reg\_FEV0.5}(x)$, $\Delta Z_{reg\_FEV1.0}(x)$ and $\tau_{reg}(x)$ are estimated in a similar way.

because no technique is available that can measure regional air content with high dynamics.

Referring to the RC model (section Mechanical Model of the Respiratory System), the start of forced expiration is given by the point at which both the global impedance (air volume) and the gradient of the global impedance (air flow) are at their maximum. In comparison to model-based data, the real-life data show a slightly different characteristic (s. Figure 6). Because the constriction and development of the maximum expiratory force do not occur in an infinitely short period of time, the proposed model is only valid after a certain point in time. Figure 6 shows that neither the point of maximal volume (maximal impedance) nor the point of maximal gradient is suitable to identify the beginning of the desired time period. The former point is too early and will lead to erroneous parameters describing fast dynamics (e.g. $FEV_{0.5}$). The latter is more suitable, but the time between this point and the end of expiration may be too short to apply robust curve fittings or other methods to determine τ_{global} and $\tau_{reg}(x)$.

For these reasons, the starting point t_{start} was defined as the mean point in time between the point of maximal impedance and the point of the maximal gradient of the impedance. Since these points are exactly the same in the proposed model, the principle of the model is not changed by this definition. The end of the considered period t_{end} is defined as the point of the lowest impedance (s. Figure 6).

Let $\Delta Z(x, t_0)$ be defined as the relative tomogram at a certain point in time t_0 with $x := (m,n)$ denoting the 2D coordinates in the tomogram. According to the definition of t_{start} and t_{end}, the EIT-based key parameters are given by

$$\Delta Z_{reg\text{-}FEV0.5}(x) = \Delta Z(x, t_{start}) - \Delta Z(x, t_{start} + 0.5\ s) \quad \text{(eq. 18)}$$

$$\Delta Z_{reg\text{-}FEV1.0}(x) = \Delta Z(x, t_{start}) - \Delta Z(x, t_{start} + 1.0\ s) \quad \text{(eq. 19)}$$

and

$$\Delta Z_{global-FEV0.5} = \int_x \Delta Z_{reg-FEV0.5}(x)\, dx \quad \text{(eq. 20)}$$

$$\Delta Z_{global-FEV1.0} = \int_x \Delta Z_{reg-FEV1.0}(x)\, dx \quad \text{(eq. 21)}$$

As explained above, the τ_{global} and $\tau_{reg}(x)$ can be derived in different ways. Here, the time constants are calculated by fitting an exponential curve to the global and regional EIT data. Hence, τ_{global} and $\tau_{reg}(x)$ are given by

$$\left\| \int_x \Delta Z(x,t)dx - \int_x \Delta Z(x,t_{start})dx \cdot \left(1 - e^{-t/\tau_{global}}\right) \right\| \xrightarrow[\forall\, t]{min} \tau_{global} \quad \text{(eq. 22)}$$

$$\left\| \Delta Z(x,t) - \Delta Z(x,t_{start}) \cdot \left(1 - e^{-t/\tau_{reg}(x)}\right) \right\| \xrightarrow[\forall\, t]{min} \tau_{reg}(x) \quad \text{(eq. 23)}$$

3. Results

In our 7 patients, the total flow resistance varies considerably. Therefore, relative changes in resistance R_{ref} measured by body plethysmography are compared with relative changes in the time constant τ_{global} based on EIT. Figure 7 plots the changes in these patients and shows that the changes in both parameters correlate well with each other.

Although the patients differed with regard to body size, weight and age, after lysis therapy the changes in flow resistance and in time constant show a reasonably good correlation (correlation coefficient r=0.879, Figure 7). Certainly, more studies should be performed to show that τ_{global} correlates linearly with the flow resistance R (here: reference R_{Ref}), a significant relationship between these two parameters seems to exist. Therefore we postulate furthermore that regional time constants $\tau_{reg}(x)$ relate to regional flow resistances during forced expiration.

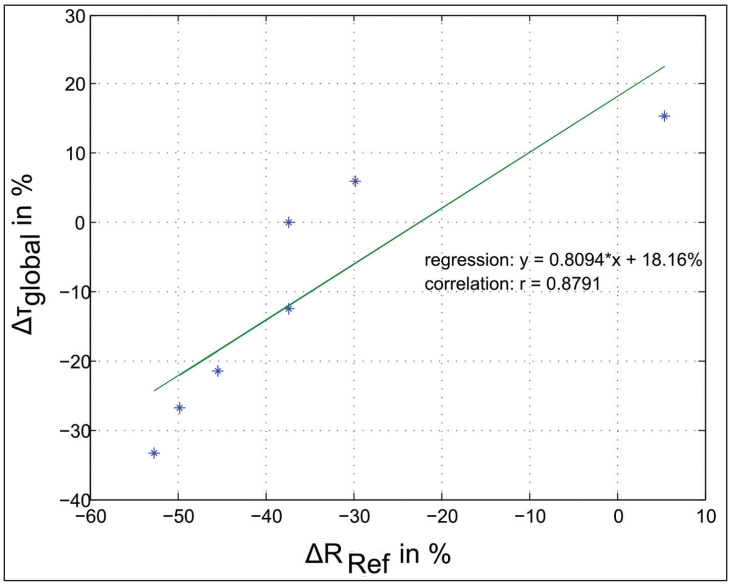

Figure 7: For the 7 study participants, changes in global time constant $\Delta\tau_{global}$ based on EIT show a good correlation with changes in flow resistance ΔR_{Ref} measured by body plethysmography (as a reference).

3.1 Regional analysis in a representative case study

Although EIT reliably estimates changes in lung air content, the routinely used techniques measure flow directly and may therefore provide more accurate assessment of global volume. However, in contrast to spirometric measurements, the great advantage of EIT is its ability to provide global and especially regional data on ventilation-related parameters.

To illustrate this, we discuss one of the 7 patients in more detail. In the absence of a gold standard to monitor regional ventilation with sufficient temporal resolution, we are only able to compare the EIT based parameters acquired before and after lysis therapy.

This male patient was aged 11 years, suffered from diagnosed asthma, and showed a significant reaction to lysis therapy with Salbutamol:

- FVC increased from 2.2 L to 2.3 L
- flow resistance decreased from 0.74 kPa·s/L to 0.42 kPa·s/L (a loss of 43.2%)
- FEF_{75} increased from 2.78 L/s to 4.61 L/s (a gain of 66 %)
- FEF_{50} increased from 1.78 L/s to 2.91 L/s (a gain of 63 %)
- FEF_{25} increased from 1.13 L/s to 1.62 L/s (a gain of 43 %)

With EIT, this response can also be demonstrated in corresponding tomograms $\Delta Z_{reg\text{-}FVC}$, $\Delta Z_{reg\text{-}Fev0.5}$ and $\Delta Z_{reg\text{-}FEV\text{-}1.0}$. In addition, the spatial distribution of gain due to the lysis therapy can be seen. To calculate the regional time constant robustly, only regional signals with a sufficient strong signal-amplitude can be considered. We consider x with

$$\Delta Z_{reg-FVC}(x, t_{start}) \geq 0.1 \cdot \max_{\forall x} \Delta Z_{reg-FVC}(x, t_{start}) \,.$$

(eq. 24)

Figure 8 shows that the total and regional gain of functional vital capacity is reflected in the corresponding gain in global and regional impedance. The difference images show that the increase of functional vital capacity is mainly distributed in the right ventral quadrant and the left dorsal quadrant (note that the left side of the tomogram represents the right side of the patient). Ventilation in the lungs show a relatively homogeneous distribution.

During the first 0.5 s, EIT presents more specific information (Figure 9). Although the

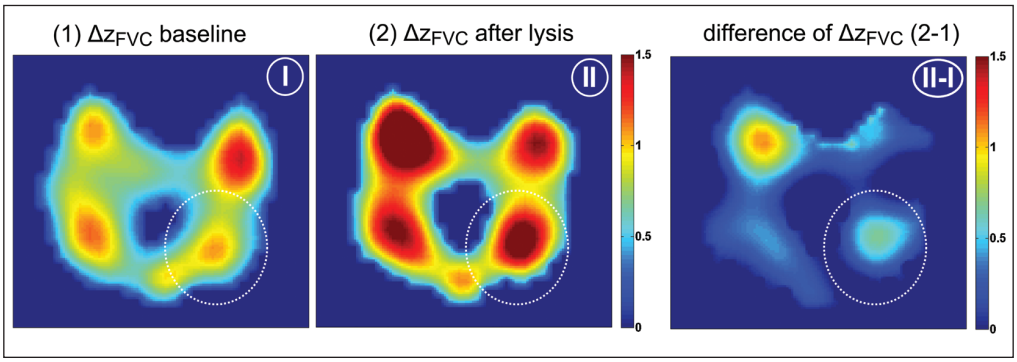

Figure 8: Relative impedance corresponding to FVC before (I) and after (II) lysis therapy. The gain is also shown (II-I): a considerable increase in air content is shown in the left dorsal quadrant (sketched area) and the right ventral quadrant.

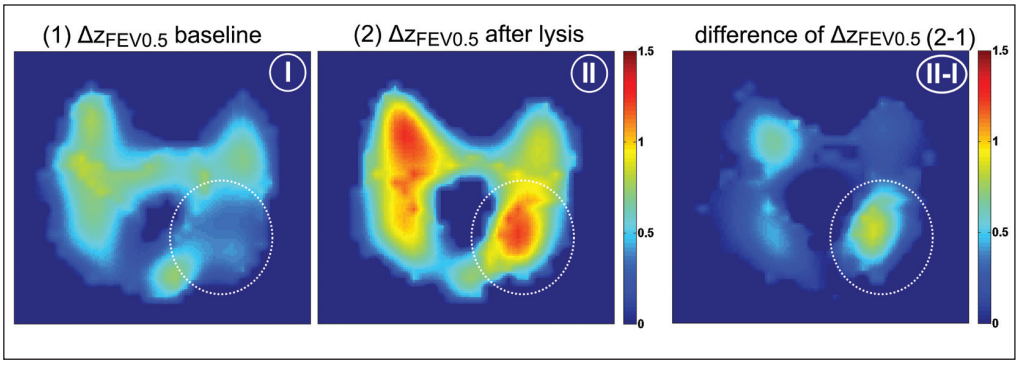

Figure 9: Impedance corresponding to the FEV0.5 before (I) and after (II) lysis therapy. The gain in expired volume (i.e. corresponding drop in impedance) after 0.5 s is also shown (II-I). Note that the distribution of the gain is different from the gain in FVC. Especially in the left dorsal part, a significantly higher change in impedance can be seen. Hence, lysis therapy facilitates faster expiration in this particular region.

left dorsal quadrant of the lung shows almost the same impedance (Figure 8 left, baseline), before lysis therapy the patient is barely able to breathe out this volume during 0.5 s (Figure 9 left, baseline); therefore, the change of impedance is almost zero in this part. After lysis therapy (Figure 9, II), this quadrant shows a significant change in impedance during the first 0.5 s. Thus, the speed of potential expiration in this region is increased, i.e. the flow resistance is significantly smaller than before.

Figure 10 shows the drop in impedance during the first 1.0 s. Whereas the patient was unable to exhale the air content in the left dorsal part of the lungs during the first 0.5 s, he is able to empty the lungs within 1.0 s relatively homogeneously (to some extent). After lysis the patient shows a greater drop in impedance compared to the drop before lysis (Figure 10, II). This was expected due to the increased global and regional functional vital capacity. Interestingly, the distribution of gain due to lysis has changed. The gain in the right ventral quadrant is about the same as that in the left dorsal quadrant. Although, the acquired functional pulmonary tissue in the right ventral quadrant is evident, this tissue does not have the same low dynamic before lysis as the left dorsal quadrant. Therefore,

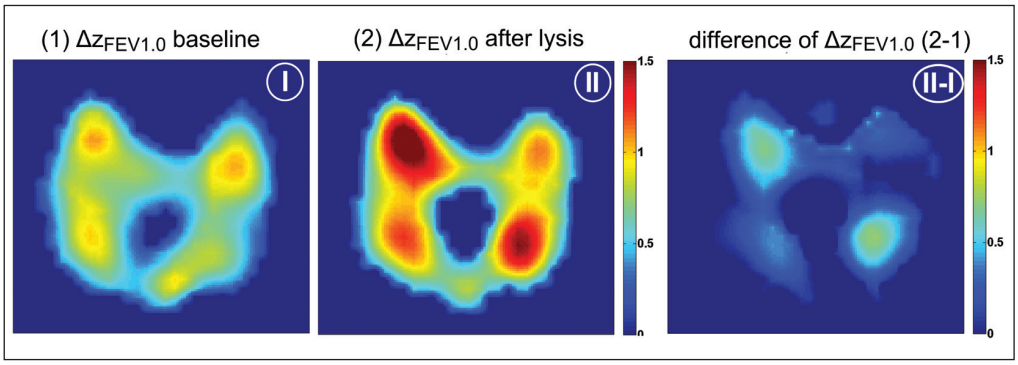

Figure 10: Impedance corresponding to the FEV1.0 before (I) and after (II) lysis therapy. The gain of expired volume (i.e. the corresponding drop in impedance) after 1.0 s is shown (II-I); note that gain in the left dorsal quadrant (sketched area) is almost the same as that in the right ventral quadrant.

the gain in relation to flow resistance was less significant.

These findings are represented in the proposed RTC map, which contains all the regional time constants $\tau_{reg}(x)$. For the patient discussed here, Figure 11 shows that the lungs had relatively low dynamics, i.e. a relatively high flow resistance before therapy (Figure 11, I). The RTC in the left lung was around 0.7 s in a relatively large area. After lysis therapy, the RTC showed a significant decrease. According to the observations in $\Delta Z_{reg\text{-}FEV0.5}$ and $\Delta Z_{reg\text{-}FEV1.0}$, the acquisition of fast lung tissue and the decrease of regional flow resistance can clearly be seen by analyzing the proposed RTC map.

4. Conclusion and outlook

Electrical impedance tomography (EIT) is a relatively new technique that is mainly used for ventilation monitoring in clinical research. Its temporal resolution is considerably better than other tomographic techniques. Due to EIT's ability to monitor temporal dynamics, new methods of analysis and parameters to

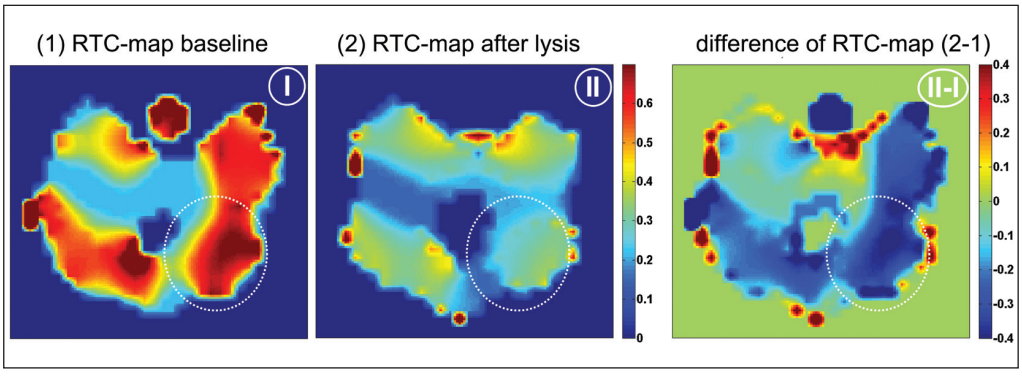

Figure 11: Regional time constant maps (RTC-maps) obtained by curve fitting during forced expiration. Overall, a considerable decrease of the regional time constant $\tau_{reg}(x)$ and, thus, reduced flow resistance in the lungs can be seen. Especially the left side shows a reduced $\tau_{reg}(x)$ of 0.3 s in a wide area. This finding is consistent with the decrease in global flow resistance R_{ref} due to lysis therapy.

describe the state of pulmonary tissue can be developed.

We have introduced the concept of regional time constant (RTC) maps to characterize the mechanical properties of pulmonary tissue and provide information on pathological modifications. In general, the time constant τ is given by the product of a flow resistance and the compliance. A model of the respiratory system during forced expiration maneuvers has demonstrated that τ builds a linear relationship with flow resistance *R* in the peripheral bronchioles. EIT provides not only global but also regional information about the filling status of pulmonary tissue. Therefore, we compared the EIT-based global time constant τ_{global} with the conventional spirometric and body plethysmographic measurement R_{Ref}. The regional distribution of $\tau_{reg}(x)$ in the lung was also investigated. The comparisons and analyses were performed before and after lysis therapy.

The study shows that changes in the flow resistance R_{ref} measured with bodyplethysmography correlate well with τ_{global} based on global impedance from EIT r=0.879. Therefore, EIT can be used in addition to, or even instead of, spirometric measurements. Because global impedance provides information similar to that provided by spirometry, it may provide similar information about a patient's health status.

Totally new information is generated when regional distribution of $\tau_{reg}(x)$ is taken into account. Currently, no technique is available that can determine regional flow resistance $R(x)$ or a regional parameter correlating to $R(x)$. Even highly developed techniques are unable to monitor fast dynamics regionally, which is necessary in order to calculate the RTC. Therefore, we can only discuss the regional distribution of $\tau_{reg}(x)$ and the regional changes in impedance at certain points in time ($\Delta Z_{reg\text{-}FEV1.0}$, $\Delta Z_{reg\text{-}FEV0.5}$ and $\Delta Z_{reg\text{-}FVC}$). The RTC-map in Figure 11 clearly shows the regional reduction of flow resistance. On the patient's left side $\tau_{reg}(x)$ shows a significant decrease of up to $\Delta\tau_{reg}(x)$=-0.4 *s*. The use of EIT in combination with spirometric measurements (or even without additional measurements) may help in the diagnosis of regional pathology. This regional information may help in the administration of lung therapy or to detect regional obstructions, which can then be screened using invasive and/or more expensive techniques (e.g. CT or MRI).

We conclude that EIT may become an important tool in the diagnosis of lung function. EIT appears to provide global information similar to that yielded by classical spirometry or body plethysmography, but also provides local information that was not previously available. The introduction of new regional time constant (RTC) maps may enable to visualize the local effects of therapy in patients with obstructive lung disease.

5. Acknowledgements

The authors thank Draeger Medical GmbH (Luebeck, Germany) for providing an EIT evaluation kit (EEK2) for the patient trial.

References

1. Barber D, Brown B. Applied potential tomography: possible clinical applications. Clinical Physics and Physiological Measurements 1985; 6: 109-121
2. Gabriel C, Peyman A, Grant E. Electrical conductivity of tissue at frequencies below 1 MHz. Phys Med Biol 2009; 54: 4863-4878
3. Frerichs I, Hahn G, Hellige G. Thoracic electrical impedance tomographic measurements during volume controlled ventilation-effects of tidal volume and positive end-expiratory pressure. IEEE Transactions on Medical Imaging 1999; 18 (9): 764-773
4. Meier T, Luepschen H, Karsten J, Leibecke T, Großherr M, Gehring H, Leonhardt S. Assessment of regional lung recruitment and derecruitment during a PEEP trial based on electrical impedance tomography. Intensive Care Med 2008; 34: 543-550
5. Wolf G, Arnold J. Electrical impedance tomography: ready for prime time? Intensive Care Med 2006; 32: 1290-1292
6. Wolf G, Grychtol B, Boyd T, Zurakowski D, Arnold J. Regional overdistension identified

with electrical impedance tomography in the perflubron-treated lung, Physiol Meas 2010; 31: 85-95
7. Frerichs I, S. P, Elke G, Reifferscheid F, Schaedler D, Weiler N. Assessment of changes in distribution of lung perfusion by electrical impedance tomography. Clin. Investigation: Respiration 2009; 77: 282-291
8. Deibele J, Luepschen H, Leonhardt S. Dynamic separation of pulmonary and cardiac changes in electrical impedance tomography. Physiol Meas 2008; 29: 1-14
9. Fagerberg A, Stenqvist O, Aneman A. Monitoring pulmonary perfusion by electrical impedance tomography: an evaluation in a pig model. Acta Anaesthesiol Scand 2009; 53: 152-158
10. Filbrun A, Popova A, Linn M, McIntosh N, Hershenson M. Longitudinal measures of lung function in infants with bronchopulmonary dysplasia. Pediatric Pulmonology 2011; 46: 369-375
11. Leonhardt S, Ahrens P, Kecman V. Analysis of tidal breathing flow volume loops for automated lung-function diagnosis in infants. IEEE Trans. on Biomedical Engineering 2010; 57: 1945-1953
12. Pillow J, Frerichs I, Stocks J. Lung function tests in neonates and infants with chronic lung disease: global and regional ventilation inhomogeneity. Pediatric Pulmonology 2006; 41: 105-121
13. Holmes J, O'Halloran R, Brodsky E, Bley T, Francois C, Velikina J, Sorkness R, Busse W, Fain S. Three-dimensional imaging of ventilation dynamics in asthmatics using multi echo projection acquisition with constrained reconstruction, Magnetic Resonance in Medicine 2009; 62: 1543-1556
14. Adler A, Arnold J, Bayford R, Borsic A, Brown B, Dixon P, Faes T, Frerichs I, Gagnon H, Gaerber Y et al. GREIT: a unified approach to 2D linear EIT reconstruction of lung images. Physiol Meas 2009; 30: 35-55
15. Barber D, Brown B. Applied potential tomography: possible clinical applications. Clinical Physics and Physiological Measurements 1985; 6: 109-121
16. Barber D. A review of image reconstruction techniques for electrical impedance tomography. Med Phys 1989; 16 (2): 162-169
17. Yorkey T, Webster J, Tompkins W. Comparing reconstruction algorithms for electrical impedance tomography. IEEE Trans. on Biomedical Engineering 1987; 34 (2): 843-852
18. Bayford R, Kantartzis P, Tizzard A, Yerworth R, Liatsis P, Demosthenous A. Development of a neonate lung reconstruction algorithm using a wavelet AMG and estimated boundary form. Physiol Meas 2008; 29: 125-138
19. Hahn G, Just A, Dudykevych T, Frerichs I, Hinz J, Quintel M, Hellige G. Imaging pathologic pulmonary air and fluid accumulation by functional and absolute EIT. Physiol Meas 2006; 27: 187-198
20. Pride N, Permutt S, Riley R, Bromberger-Barnea B. Determinants of maximal expiratory flow from the lungs. J of appl Physiology 1967; 23 (5): 646-662
21. Mead J, Turner J, Macklem P, Little J. Significance of the relationship between lung recoil and maximum expiratory flow. J Appl Physiol 1967; 22 (1): 95-108
22. Fry D. Theoretical Considerations of the Bronchial Pressure-Flow-Volume Relationship with particular reference to the maximum expiratory flow volume curve. Phys Med Biol 1958; 3: 174-194
23. Hinz J, Neumann P, Dudykevych T, Andersson L, Wrigge H, Burchardi H, Hedenstierna G. Regional ventilation by electrical impedance tomography: a comparison with ventilation scintigraphy in pigs. Chest 2003; 124: 314-322
24. Frerichs I, Hinz J, Herrmann P, Weisser G, Hahn G, Dudykevych T, Quintel M, Hellige G. Detection of local lung air content by electrical impedance tomography compared with electron beam CT. J Appl Physiol 2002; 93: 660-666
25. Hahn G, Sipinkova I, Baisch F, Hellige G. Changes in the thoracic impedance distribution under different ventilatory conditions. Physiol Meas 1995; 16: 161-173
26. Frerichs I, S. P, Elke G, Reifferscheid F, Schaedler D, Weiler N. Assessment of changes in distribution of lung perfusion by electrical impedance tomography. Clin. Investigation: Respiration 2009; 77: 282-291

Correspondence address
Dipl.-Ing. Robert Pikkemaat
Philips Chair for Medical Information Technology
RWTH Aachen
Pauwelsstr. 20
52074 Aachen
Germany
pikkemaat@hia.rwth-aachen.de